PHYSICAL REVIEW B **88**, 020402(R) (2013)

Unraveling the origins of electromechanical response in mixed-phase bismuth ferrite

R. K. Vasudevan,[1,*,†] M. B. Okatan,[1,*,†] Y. Y. Liu,[2] S. Jesse,[3] J.-C. Yang,[4] W.-I. Liang,[4]
Y.-H. Chu,[4] J. Y. Li,[5] S. V. Kalinin,[3,‡] and V. Nagarajan[1,§]

[1]*School of Materials Science and Engineering, University of New South Wales, Kensington 2052, Australia*
[2]*Faculty of Materials, Optoelectronics and Physics, and Key Laboratory of Low Dimensional Materials & Application Technology of Ministry of Education, Xiangtan University, Xiangtan, Hunan 411105, China*
[3]*The Center for Nanophase Materials Sciences, Oak Ridge National Laboratory, Oak Ridge, Tennessee 37831, USA*
[4]*Department of Materials Science and Engineering, National Chiao Tung University, Hsinchu 30010, Taiwan*
[5]*Department of Mechanical Engineering, University of Washington, Seattle, Washington 98195-600, USA*

(Received 11 September 2012; published 8 July 2013)

The origin of giant electromechanical response in a mixed-phase rhombohedral-tetragonal $BiFeO_3$ thin film is probed using subcoercive scanning probe microscopy based multiple-harmonic measurements. Significant contributions to the strain arise from a second-order harmonic response localized at the phase boundaries. Strain and dissipation data, backed by thermodynamic calculations, suggest that the source of the enhanced electromechanical response is the motion of phase boundaries. These findings elucidate the key role of labile phase boundaries, both natural and artificial, in achieving thin films with giant electromechanical properties.

DOI: 10.1103/PhysRevB.88.020402 PACS number(s): 77.55.Px, 77.80.bn, 77.80.Dj

The recent discovery of a strain-induced morphotropic phase boundary (MPB) in epitaxial bismuth ferrite [$BiFeO_3$ (BFO)] thin films[1] with a giant piezoelectric response[2] as well as electrically switchable spontaneous magnetism[3] has triggered immense scientific interest. Experiments thus far reveal this system to contain a rich tapestry of phases and interfaces[4–8] and hint at a variety of mechanisms (e.g., polarization rotation, electrostriction, and phase boundary motion) behind the enhanced piezoelectric response. However, none provide a direct and complete picture. Theoretically, Roytburd *et al.*[9] propose that the large response found in mixed-phase films arises from properties manifesting from elastic interactions between heterophase domains; particularly, elastic interactions lower energy barriers between competing phases, increasing the mobility of phase boundaries. Indeed, the significance of the motion of artificially created phase boundaries has been demonstrated.[10] It follows that unraveling the direct role of the interfaces such as nanoscale phase boundaries is required to understand the origins of the unique functionality of this materials system, especially given that novel properties often localize at the interface.[11,12] This knowledge also underpins mechanisms that control the behavior of a wide class of disordered materials such as relaxors,[13] martensites,[14] strain glasses,[15] and polar oxides.[16]

In this Rapid Communication, multiple-harmonic scanning probe microscopy (SPM) and thermodynamic calculations are exploited in a complementary fashion to decipher the origins of enhanced electromechanical response in mixed-phase $BiFeO_3$ thin films. By quantitatively probing the first- and second-order harmonics of strain and dissipation with band-excitation SPM methods,[17,18] competing contributions are decoupled and mapped spatially with nanometer precision. A Rayleigh-type model is then developed to explain the experimental observations. The results show that activated phase boundary motion is the source of enhanced piezoelectric response at low fields, as opposed to other intrinsic effects such as polarization rotations. This provides direct experimental evidence of the nanoscale origins of enhanced piezoelectric response in mixed-phase BFO. Furthermore, this approach can be extended to other polycrystalline and polydomain ferroelectrics in order to grasp the role of such extrinsic contributors[19–23] in their electromechanical response.

Figure 1 outlines the possible sources of enhancement including interfacial mechanisms, i.e., reversible and irreversible motion of phase boundaries,[24] and lattice contributions arising from polarization rotation[25,26] or electrostriction.[27,28] Importantly, while indistinguishable in linear theory, these mechanisms give rise to markedly different nonlinear behaviors.[29–31] Whereas reversible interfacial motion and electrostriction produce second-order harmonic contributions to the strain,[27,30] the irreversible motion of an interface only contributes to odd-order harmonics. This entails that the band-excitation harmonic method can be effectively employed to unravel the respective contributions from these individual mechanisms.[18]

Experiments were carried out on a 60-nm-thick $BiFeO_3$ film grown on $LaAlO_3$ with a 5 nm $LaNiO_3$ bottom electrode using band-excitation scanning probe microscopy[17] on an Asylum Research (Cypher) microscope, and first and second harmonic responses were captured as discussed elsewhere.[18] Piezoresponse force microscopy (PFM) was used to investigate the initial domain structure of the mixed-phase film, and is shown elsewhere.[32] The topography of a 500 nm × 500 nm area is displayed in Fig. 2(a). The naming convention for the phases used by Damodaran *et al.*[33] is employed in describing the phases present, with the system consisting of a matrix of monoclinic phase M_{II}, and mixed-phase regions consisting of a tilted M_{II} phase termed $M_{II,tilt}$, along with a highly distorted phase M_I as marked in Fig. 2(a). As explained in Ref. 33, the tetragonal-like monoclinic phase is designated as M_{II}, while the rhombohedral-like monoclinic phase is M_I. Finally, the phase adjacent to the M_I phase in the mixed-phase regions is referred to as $M_{II,tilt}$. In agreement with prior reports, the M_I and $M_{II,tilt}$ phases form a corrugated network on the surface, with both phases tilted slightly with respect to the substrate (001) surface plane, as indicated in the inset in Fig. 2(a).

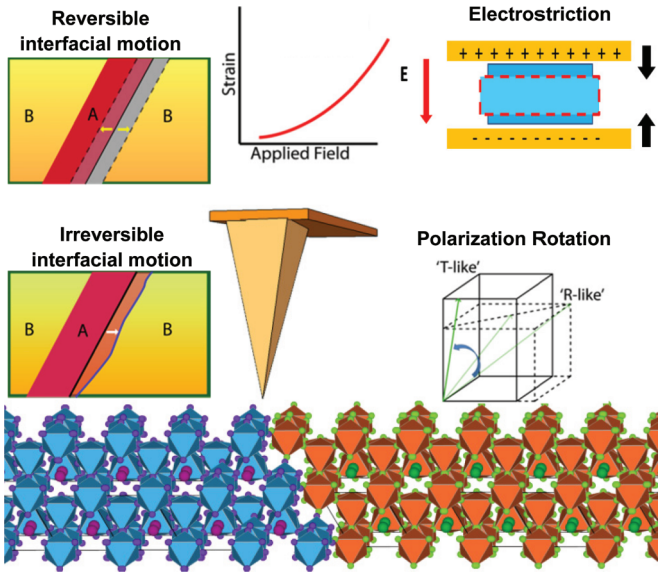

FIG. 1. (Color online) Possible sources of enhancement of piezoresponse (i.e., strain) in mixed-phase $BiFeO_3$ at subcoercive fields. The additional contributions to the strain can be categorized as arising from interfacial effects (reversible and irreversible phase boundary motion) or noninterfacial effects (polarization rotation, or electrostriction). Note that the diagram is for illustrative purposes, and the tip is not to scale.

The first and second harmonic piezoresponses (i.e., strain) were measured as a function of applied ac fields at each point in a 50 × 50 pixel grid. These measurements yield a data set of $[A,Q,\omega_r,\theta][x,y,V_{ac}]$, where A is the electromechanical amplitude, Q is the Q factor of the cantilever, ω_r is the cantilever resonance, θ is the phase of the response, x,y are the spatial coordinates, and V_{ac} is the probing voltage. The datasets for the first and second harmonic amplitudes as a function of spatial position and applied bias are given as video files.[32] Note that the response is measured in the same units, allowing direct comparison between harmonics. The datasets were then analyzed using principal component analysis (PCA), a practical method for visualizing the trends quantitatively in multidimensional datasets.[32,34] The corresponding position-dependent eigenvalues (loading maps) are shown in Figs. 2(b)–2(d). The first harmonic piezoresponse amplitude loading map in Fig. 2(b) appears to closely match the PFM image, as expected. The second harmonic piezoresponse amplitude loading map, shown in Fig. 2(c), appears to show a peak around the edge of the M_I phase, but is concentrated on the $M_{II,tilt}$ side of the phase boundary [see the schematic in Fig. 2(a)]. The trends in the dissipation are shown in the loading map in Fig. 2(d), and highlight increased dissipation near the phase boundaries. Since the spatial maps are significantly different, this highlights that there is a statistically significant variation that is linked to the microstructure of the film.

To examine whether the enhanced electromechanical response is due to bulk intrinsic mechanisms such as electrostriction and polarization rotation, thermodynamic calculations were performed following formalism developed elsewhere,[35] as detailed in the Supplemental Material.[32] For bulk rhombohedral BFO, such calculations resulted in a spontaneous polarization of 100 $\mu C/cm^2$, a d_{33} of 21 pm/V, and a dielectric constant of 97, in good agreement with both density functional theory calculations and recent experimental measurements[32] (see also Refs. 35–46 therein). Because the aim is to determine the intrinsic factors affecting the piezoelectric response, we consider each phase distinctly and neglect the contribution of domain walls in our calculations. Note that all calculations were carried out for the BFO film at room temperature, consistent with experimental conditions. The spontaneous polarization as a function of misfit strain is evaluated first, as shown in Fig. 3(a), from which the dielectric constants [Fig. 3(b)] and piezoelectric coefficients [Fig. 3(c)] are evaluated. Calculations reveal that polarization components vary continuously across MPB, though the slope of P_1 and P_2 is discontinuous at the MPB. As a result, there is a large peak in the dielectric constants ε_{31} and ε_{32} on the highly distorted M_I phase side of the MPB, but no peak on the tetragonal-like M_{II} side, or in rhombohedral BFO, shown in Fig. 3(b). Such a large dielectric constant could suggest bulk intrinsic factors to be crucial in enhancing the strain response, yet the piezoelectric coefficient at the MPB was calculated to be only 12 pm/V, much smaller than experimental observation, despite the fact that the same calculation leads to ferroelectric and electromechanical properties that are in good agreement with experiments for a bulk rhombohedral phase.[32] Indeed, as a first estimate, the strain calculated in this fashion can only account for ∼65% of the experimentally observed strain through PFM.[32] Moreover, other experimental evidence suggests that these bulk intrinsic mechanisms are not the only factors governing the response of the mixed-phase system, for several reasons. First, the second harmonic amplitude peaks near the phase boundary, and not in the M_I phase as would be expected (i.e., spatial mapping reveals confinement to interfacial regions rather than the whole phase). Second, the magnitude of the second harmonic signal itself is at least 65% that of the first harmonic at 2.5 V [Figs. 4(b) and 4(d)], while the total strain calculated from intrinsic mechanisms[32] [Fig. 3(d)] is almost linear with applied field, despite the consideration of nonlinear responses from bulk intrinsic processes such as electrostriction and polarization rotation. Furthermore, the amplitude in the piezoelectric response is in fact highest on the $M_{II,tilt}$ side of the phase boundary, while the thermodynamically calculated strain is highest on the rhombohedral side and lowest on the M_{II} side, at odds with the data. Additionally, electrostriction is a nondissipative process, which contradicts dissipation data [Fig. 2(d)], which shows a significant correlation between the emergence of the second harmonic signal and increased dissipation. Due to these conflicts, intrinsic processes cannot adequately explain the data without incorporation of the effects of the domain walls in the material.

To explore the role of the domain wall in this system, we present a phenomenological Rayleigh-type model to rationalize the effect of the interfacial contribution by the domain walls. The model of reversible phase boundary motion, termed "dynamic poling" by Bassiri-Gharb *et al.*,[29,30] is extended in explaining the harmonic contributions to the strain response. The applied field by the SPM tip is sinusoidal with amplitude E_0, i.e., $E_{ac} = E_0 \sin(\omega t)$, and the total strain induced by the

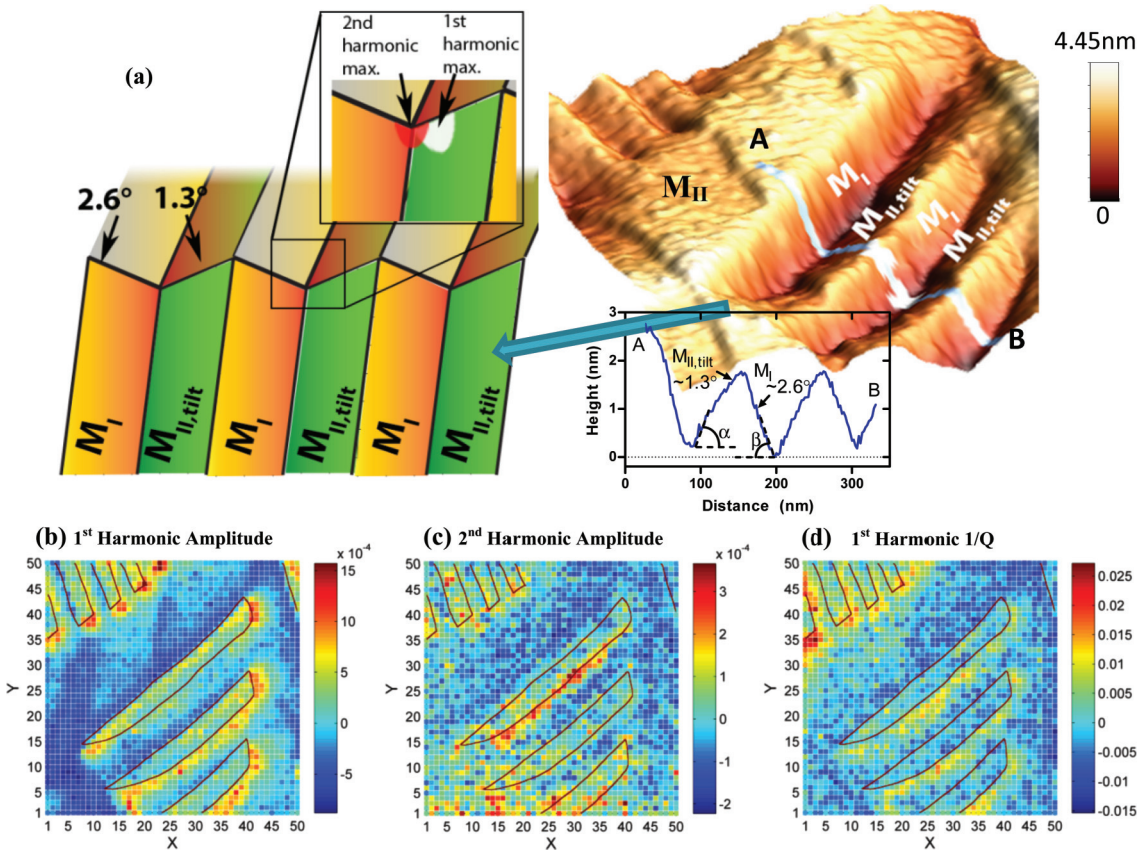

FIG. 2. (Color online) First and second harmonic responses. (a) Topography (right) and schematic (left) of a 500 nm × 500 nm region of the mixed-phase $BiFeO_3$ film. A line profile is also shown to indicate the angles α,β that the M_I and $M_{II,tilt}$ phases make with respect to the substrate (001) surface plane. The area was split into a 50 × 50 grid and the piezoresponse (first and second harmonic) and dissipation ($1/Q$) were captured at each point in the grid. A PCA of the piezoresponse and dissipation datasets was performed, with loading maps shown for the first eigenvector for (b) first harmonic piezoresponse amplitude, (c) second harmonic piezoresponse amplitude, and (d) first harmonic dissipation ($1/Q$). For (b)–(d), the boundaries of the M_I phase [as determined from (a)] are overlaid as black outlines.

electric field can be written as $S = QP_{\text{total}}^2 - QP_s^2$, where Q is the electrostriction coefficient, P_{total} is the sum of the spontaneous polarization P_s and the polarization which is induced by the electric field, which can be decomposed into two components, P_{re}, which is reversible polarization under ac electric field, and P_{ir}, which is associated with irreversible movements of the phase boundary, i.e., $P_{\text{total}} = P_s + P_{\text{re}} + P_{\text{ir}}$. P_s can be calculated by thermodynamic methods. It is further assumed that the reversible and irreversible polarization terms can be expressed in terms of standard Rayleigh relationships for reversible and irreversible contributions (consistent with the "dynamic poling" model), i.e.,

$$\begin{aligned} P_{\text{re}} &= \varepsilon_0\chi_0\left[1+\beta\sin(\omega t)\right]E_{\text{ac}} \\ &= \varepsilon_0\chi_0 E_0\sin(\omega t) + \varepsilon_0\chi_0 E_0\beta\sin^2(\omega t), \end{aligned} \tag{1}$$

$$\begin{aligned} P_{\text{ir}} &= \alpha_\varepsilon E_0 E_{\text{ac}} \pm \frac{\alpha_\varepsilon}{2}\left(E_0^2 - E_{\text{ac}}^2\right) \\ &= \alpha_\varepsilon E_0^2\sin(\omega t) \pm \frac{\alpha_\varepsilon}{2}E_0^2\cos^2(\omega t), \end{aligned} \tag{2}$$

where ε_0 is the dielectric constant of free space, χ_0 is the relative dielectric constant related to the phase structure, β is a scaling factor for the frequency dependence of the reversible polarization P_{re}, and α_ε is the irreversible polarization Rayleigh coefficient. Using these relations, the equation for the strain S can then be developed by Fourier expansion.[32] Since the nonlinearity observed is in fact small in this system,[32] the expressions for the strain, for the first and second harmonics $S_{1\text{st}}$ and $S_{2\text{nd}}$, become

$$S_{1\text{st}} \cong \frac{4QP_s\varepsilon_0\chi_0E_0 + 3Q\beta\varepsilon_0^2\chi_0^2E_0^2}{2}\sin(\omega t), \tag{3}$$

$$S_{2\text{nd}} \cong -\frac{8QP_s\beta\varepsilon_0\chi_0E_0 + 4Q(1+\beta^2)\varepsilon_0^2\chi_0^2E_0^2}{8}\cos(2\omega t). \tag{4}$$

Equations (3) and (4) indicate the changes in polarization in the system from purely reversible processes. Equation (4) consists of the two distinct processes that contribute to the second harmonic, electrostriction ($\sim Q\varepsilon_0^2\chi_0^2$), and the contribution from reversible phase boundary motion (all terms involving β).

Notably, in the case where $\varepsilon_0\chi_0$ is large, as is the case for the mixed-phase bands, the contribution from reversible phase boundary motion is likely to be significantly larger as well. In this sense the large response from reversible interfacial motion stems not only from the labile walls, but from the intrinsically large dielectric constants on the M_I side of the MPB. It is this

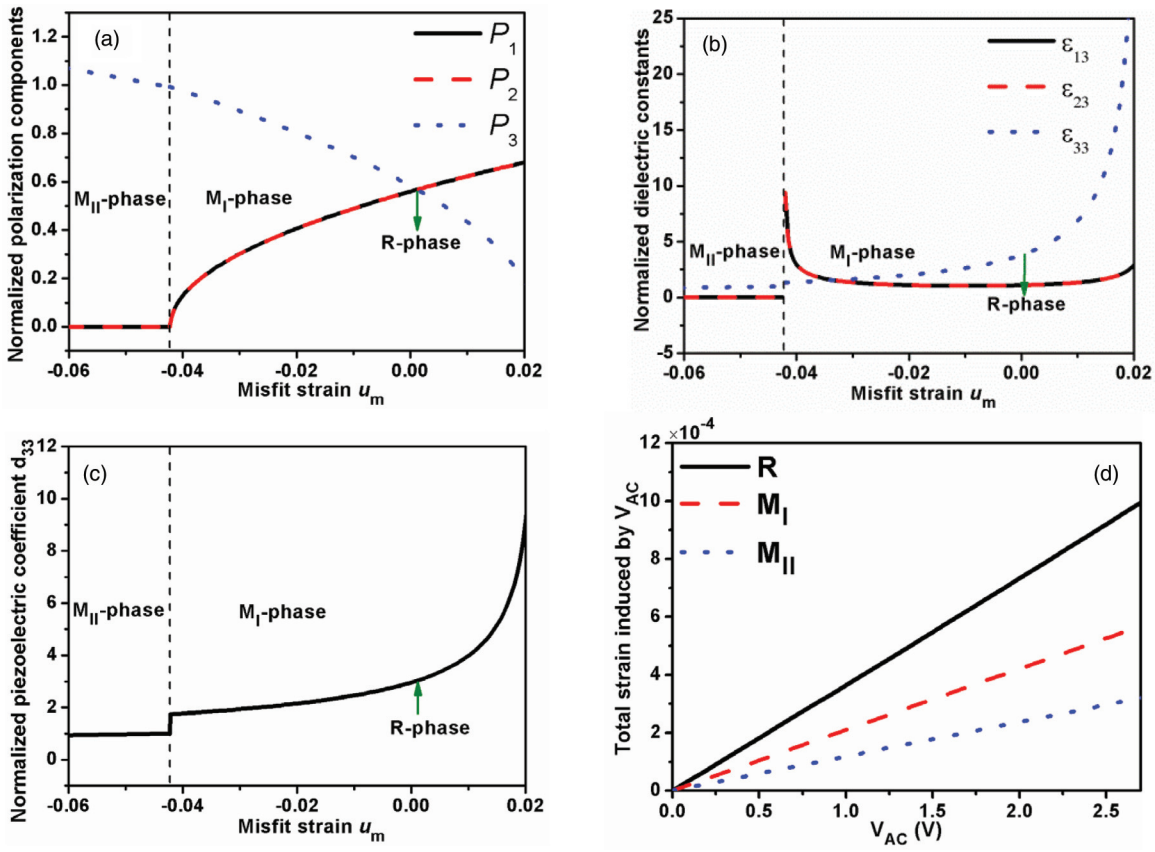

FIG. 3. (Color online) Thermodynamic calculations. (a) Polarization, (b) dielectric constants, and (c) piezoelectric coefficients vs the misfit strain; (d) the total strain induced by the applied ac bias for different phases.

combination of these two factors that leads to a significant second harmonic contribution to the strain.

To confirm whether the model of reversible phase boundary motion accurately explains the experimental observations, the captured data was reanalyzed through a regional deconstruction to correlate the measured responses with the observed phases. This capability to identify spatial variability of measured responses and correlate it with the microstructure is a unique aspect of SPM. The area was split into the three distinct phases, as shown in Fig. 4(a). This deconstruction was achieved by using the surface topography (deflection) image.[32] The average piezoresponse amplitude and dissipation ($1/Q$) for the first and second harmonics for the three regions as a function of applied ac bias are plotted in Figs. 4(b)–4(e), respectively. Note that the error in the data points is extremely small.[32] The first four points in the first harmonic response and the first 12 points in the second harmonic response are excluded (marked "weak signal region") from analysis due to poor signal in these voltage ranges. The graph in Fig. 4(b) shows that the mixed-phase regions display a significantly higher piezoresponse than the surrounding matrix phase. The piezoresponse amplitude is also found to deviate from linearity in a transition range 0.85–$1.18V_{ac}$,[32] and is indicated by the gray shaded region. Additionally, the dependency of the dissipation on the probing bias, in Fig. 4(c), indicates that there exists significantly higher dissipation in the mixed-phase bands. Interestingly, at the same transition voltage range, the trends for the M_{II} and mixed-phase regions diverge. This can be rationalized by assuming that the dissipation up to $\sim 1V_{ac}$ is very similar for the three phases due to intrinsic and instrumental losses, but that beyond $\sim 1V_{ac}$, the phase boundary motion is activated, and begins moving, leading to greater dissipation and, additionally, larger strain. The fact that the divergence occurs at the same voltage range at which a deviation in the first harmonic piezoresponse is observed is evidence that the same mechanism is responsible for both observations. More specifically, the divergence from linearity in the first harmonic and the emergence of the second harmonic can be rationalized by considering that for low applied fields, the contribution from domain walls [β in Eqs. (3) and (4)] is zero, due to pinning. When the field is large enough, the walls become depinned, leading to nonzero β, resulting in increased first harmonic response and emergence of a second harmonic signal, thus explaining the observed data. This contribution from the interface also results in higher dissipation, which is again observed in the vicinity of the phase boundaries. Note that the M_{II} phase has a striped domain structure with monoclinic walls;[47,48] thus second harmonic contributions can be expected from the motion of such walls also, but these appear to be weaker, as indicated in Fig. 4(d).

In summary, through SPM band-excitation harmonic experiments, backed by thermodynamic calculations, it is shown that the origin of large piezoresponse in mixed-phase epitaxial $BiFeO_3$ films at subcoercive voltage is the activated motion of the labile phase boundaries. By employing a modified Rayleigh-type model, it is found that the activated, reversible

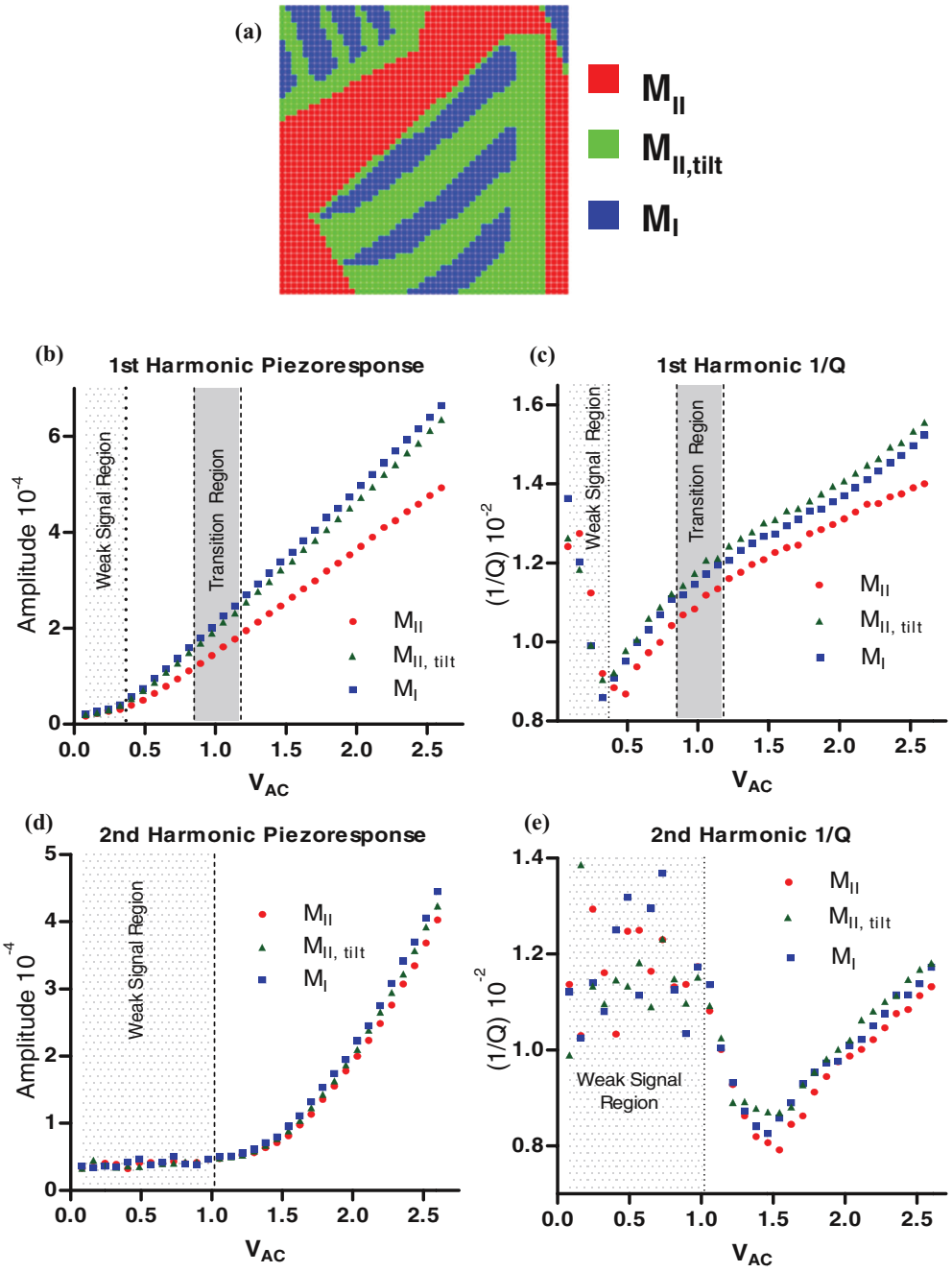

FIG. 4. (Color online) Regional deconstruction, showing differences in average response in the three regions: the matrix M_{II} phase (red), and the mixed-phase regions consisting of $M_{II,tilt}$ phase (green) and M_I phase (blue). (a) Regional deconstruction map. (b) Average first harmonic piezoresponse and (c) dissipation $(1/Q)$ for the three phases. (d) Average second harmonic piezoresponse and (e) dissipation $(1/Q)$ for all three phases. The "weak signal region" is shaded in (b)–(e); these data points are dominated by noise and can be neglected. Plots with error bars are provided elsewhere (Ref. 32).

motion of the phase boundaries result in large second- and higher-order contributions to the strain, consistent with strain and dissipation data at low fields. Other possible contributions to the strain are studied, but are found to be inconsistent with experimental observations. These results shed light on the origins of the large electromechanical response in mixed-phase $BiFeO_3$ films, and highlight the crucial role of phase boundary motion in enhancing and optimizing electromechanical properties.

R.K.V., M.B.O., and V.N. acknowledge support from the ARC Discovery Project scheme. R.K.V. and V.N. acknowledge financial support from the Australian Nanotechnology Network. The research at ORNL (S.J. and S.V.K.) was conducted at the Center for Nanophase Materials Sciences, which is sponsored at Oak Ridge National Laboratory by the Division of Scientific User Facilities, US Department of Energy. The work at NCTU is supported by National Science Council, Taiwan (under Contract No.

NSC-101-2119-M-009-003-MY2), Ministry of Education (under Grant No. MOE-ATU 101W961), and Center for Interdisciplinary Science of National Chiao Tung University. Y.Y.L. acknowledges the support of NSFC (11102175 and 11090331), and J.Y.L. acknowledges the support of ARO (W911NF-07-1-0410).

*Current address: The Center for Nanophase Materials Sciences, Oak Ridge National Laboratory, Oak Ridge, TN 37831, USA.
†These two authors contributed equally to the manuscript.
‡sergei2@ornl.gov
§nagarajan@unsw.edu.au

[1]R. J. Zeches, M. D. Rossell, J. X. Zhang, A. J. Hatt, Q. He, C. H. Yang, A. Kumar, C. H. Wang, A. Melville, C. Adamo, G. Sheng, Y. H. Chu, J. F. Ihlefeld, R. Erni, C. Ederer, V. Gopalan, L. Q. Chen, D. G. Schlom, N. A. Spaldin, L. W. Martin, and R. Ramesh, Science **326**, 977 (2009).

[2]J. X. Zhang, B. Xiang, Q. He, J. Seidel, R. J. Zeches, P. Yu, S. Y. Yang, C. H. Wang, Y. H. Chu, L. W. Martin, A. M. Minor, and R. Ramesh, Nat. Nanotechnol. **6**, 98 (2011).

[3]Q. He, Y. H. Chu, J. T. Heron, S. Y. Yang, W. I. Liang, C. Y. Kuo, H. J. Lin, P. Yu, C. W. Liang, R. J. Zeches, W. C. Kuo, J. Y. Juang, C. T. Chen, E. Arenholz, A. Scholl, and R. Ramesh, Nat. Commun. **2**, 225 (2011).

[4]H. M. Christen, J. H. Nam, H. S. Kim, A. J. Hatt, and N. A. Spaldin, Phys. Rev. B **83**, 144107 (2011).

[5]Z. Chen, Z. Luo, C. Huang, Y. Qi, P. Yang, L. You, C. Hu, T. Wu, J. Wang, C. Gao, T. Sritharan, and L. Chen, Adv. Funct. Mater. **21**, 133 (2011).

[6]Z. Chen, S. Prosandeev, Z. L. Luo, W. Ren, Y. Qi, C. W. Huang, L. You, C. Gao, I. A. Kornev, T. Wu, J. Wang, P. Yang, T. Sritharan, L. Bellaiche, and L. Chen, Phys. Rev. B **84**, 094116 (2011).

[7]R. K. Vasudevan, Y. Liu, J. Li, W.-I. Liang, A. Kumar, S. Jesse, Y.-C. Chen, Y.-H. Chu, V. Nagarajan, and S. V. Kalinin, Nano Lett. **11**, 3346 (2011).

[8]A. R. Damodaran, S. Lee, J. Karthik, S. MacClaren, and L. W. Martin, Phys. Rev. B **85**, 024113 (2012)

[9]A. L. Roytburd, J. Ouyang, B. M. Boyerinas, and H. A. Bruck, Appl. Phys. Lett. **99**, 172902 (2011).

[10]Y. Bastani and N. Bassiri-Gharb, Acta Mater. **60**, 1346 (2012).

[11]E. K. H. Salje, Chem. Phys. Chem. **11**, 940 (2010).

[12]J. Seidel, L. W. Martin, Q. He, Q. Zhan, Y. H. Chu, A. Rother, M. E. Hawkridge, P. Maksymovych, P. Yu, M. Gajek, N. Balke, S. V. Kalinin, S. Gemming, F. Wang, G. Catalan, J. F. Scott, N. A. Spaldin, J. Orenstein, and R. Ramesh, Nat. Mater. **8**, 229 (2009).

[13]V. Westphal, W. Kleemann, and M. D. Glinchuk, Phys. Rev. Lett. **68**, 847 (1992).

[14]R. Ahluwalia and G. Ananthakrishna, Phys. Rev. Lett. **86**, 4076 (2001).

[15]S. Sarkar, X. Ren, and K. Otsuka, Phys. Rev. Lett. **95**, 205702 (2005).

[16]A. Ohtomo and H. Y. Hwang, Nature (London) **427**, 423 (2004).

[17]S. Jesse, S. V. Kalinin, R. Proksch, A. P. Baddorf, and B. J. Rodriguez, Nanotechnology **18**, 435503 (2007).

[18]Y. Kim, A. Kumar, A. Tselev, I. I. Kravchenko, H. Han, I. Vrejoiu, W. Lee, D. Hesse, M. Alexe, S. V. Kalinin, and S. Jesse, ACS Nano **5**, 9104 (2011).

[19]D. Damjanovic, J. Appl. Phys. **82**, 1788 (1997).

[20]A. Pramanick, D. Damjanovic, J. C. Nino, and J. L. Jones, J. Am. Ceram. Soc. **92**, 2291 (2009).

[21]J. Karthik, A. R. Damodaran, and L. W. Martin, Phys. Rev. Lett. **108**, 167601 (2012).

[22]G. Tutuncu, D. Damjanovic, J. Chen, and J. L. Jones, Phys. Rev. Lett. **108**, 177601 (2012).

[23]R. K. Vasudevan, M. B. Okatan, C. Duan, Y. Ehara, H. Funakubo, A. Kumar, S. Jesse, L.-Q. Chen, S. V. Kalinin, and V. Nagarajan, Adv. Funct. Mater. **23**, 81 (2013).

[24]F. Xu, S. Trolier-McKinstry, W. Ren, B. Xu, Z. L. Xie, and K. J. Hemker, J. Appl. Phys. **89**, 1336 (2001).

[25]G. Xu, H. Luo, H. Xu, and Z. Yin, Phys. Rev. B **64**, 020102 (2001).

[26]J. Rouquette, J. Haines, V. Bornand, M. Pintard, P. Papet, W. G. Marshall, and S. Hull, Phys. Rev. B **71**, 024112 (2005).

[27]W. Lehmann, H. Skupin, C. Tolksdorf, E. Gebhard, R. Zentel, P. Krüger, M. Lösche, and F. Kremer, Nature (London) **410**, 447 (2001).

[28]Q. M. Zhang, V. Bharti, and X. Zhao, Science **280**, 2101 (1998).

[29]N. Bassiri-Gharb, S. Trolier-McKinstry, and D. Damjanovic, J. Appl. Phys. **110**, 124104 (2011).

[30]S. Trolier-McKinstry, N. B. Gharb, and D. Damjanovic, Appl. Phys. Lett. **88**, 202901 (2006).

[31]D. Damjanovic, in *Science of Hysteresis*, edited by G. Bertotti and I. D. Mayergoyz (Elsevier, Oxford, U.K., 2005), Vol. 3, p. 337.

[32]See Supplemental Material at http://link.aps.org/supplemental/10.1103/PhysRevB.88.020402 for additional datasets, further analysis, full derivations, and videos of captured data.

[33]A. R. Damodaran, C.-W. Liang, Q. He, C.-Y. Peng, L. Chang, Y.-H. Chu, and L. W. Martin, Adv. Mater. **23**, 3170 (2011).

[34]S. Jesse and S. V. Kalinin, Nanotechnology **20**, 085714 (2009).

[35]Y. Y. Liu, R. K. Vasudevan, K. Pan, S. H. Xie, W. I. Liang, A. Kumar, S. Jesse, Y. C. Chen, Y. H. Chu, V. Nagarajan, S. V. Kalinin, and J. Y. Li, Nanoscale **4**, 3175 (2012).

[36]N. A. Pertsev, A. G. Zembilgotov, and A. K. Tagantsev, Phys. Rev. Lett. **80**, 1988 (1998).

[37]J. Zhang, D. Schlom, L. Chen, and C. Eom, Appl. Phys. Lett. **95**, 122904 (2009).

[38]J. B. Neaton, C. Ederer, U. V. Waghmare, N. A. Spaldin, and K. M. Rabe, Phys. Rev. B **71**, 014113 (2005).

[39]P. Ravindran, R. Vidya, A. Kjekshus, H. Fjellvåg, and O. Eriksson, Phys. Rev. B **74**, 224412 (2006).

[40]S. Picozzi and C. Ederer, J. Phys.: Condens. Matter **21**, 303201 (2009).

[41]D. Lebeugle, D. Colson, A. Forget, and M. Viret, Appl. Phys. Lett. **91**, 022907 (2007).

[42]V. Shvartsman, W. Kleemann, R. Haumont, and J. Kreisel, Appl. Phys. Lett. **90**, 172115 (2007).

[43]G. Yuan and S. W. Or, Appl. Phys. Lett. **88**, 062905 (2006).

[44]R. P. S. M. Lobo, R. L. Moreira, D. Lebeugle, and D. Colson, Phys. Rev. B **76**, 172105 (2007).

[45]S. Redfern, C. Wang, J. Hong, G. Catalan, and J. Scott, J. Phys.: Condens. Matter **20**, 452205 (2008).

[46]D. Lebeugle, D. Colson, A. Forget, M. Viret, P. Bonville, J. F. Marucco, and S. Fusil, Phys. Rev. B **76**, 024116 (2007).

[47]Y.-C. Chen, Q. He, F.-N. Chu, Y.-C. Huang, J.-W. Chen, W.-I. Liang, R. K. Vasudevan, V. Nagarajan, E. Arenholz, S. V. Kalinin, and Y.-H. Chu, Adv. Mater. **24**, 3070 (2012).

[48]L. You, Z. Chen, X. Zou, H. Ding, W. Chen, L. Chen, G. Yuan, and J. Wang, ACS Nano **6**, 5388 (2012).